

2020

Theoretical Studies of Thin-Film Solar Cells based on CdTe with different Window-Layers

H. A. Mohamed

Physics department, Faculty of Science, Sohag University, 82524 Sohag, Egypt,
hussein_abdelhafez2000@yahoo.com

Mahrous R. Ahmed

Physics department, Faculty of Science, Sohag University, 82524 Sohag, Egypt,
hussein_abdelhafez2000@yahoo.com

Sh. S. Ali

Physics department, Faculty of Science, Sohag University, 82524 Sohag, Egypt,
hussein_abdelhafez2000@yahoo.com

W. S. Mohamed

*Physics department, Faculty of Science, Sohag University, 82524 Sohag, Egypt\ Physics Department,
College of Science, Jouf University, Al-Jouf, Sakaka, P.O. Box 2014, Saudi Arabia,*
hussein_abdelhafez2000@yahoo.com

Follow this and additional works at: <https://digitalcommons.aaru.edu.eg/ijtfst>

Recommended Citation

A. Mohamed, H.; R. Ahmed, Mahrous; S. Ali, Sh.; and S. Mohamed, W. (2020) "Theoretical Studies of Thin-Film Solar Cells based on CdTe with different Window-Layers," *International Journal of Thin Film Science and Technology*: Vol. 9 : Iss. 3 , Article 4.

Available at: <https://digitalcommons.aaru.edu.eg/ijtfst/vol9/iss3/4>

This Article is brought to you for free and open access by Arab Journals Platform. It has been accepted for inclusion in International Journal of Thin Film Science and Technology by an authorized editor. The journal is hosted on [Digital Commons](#), an Elsevier platform. For more information, please contact rakan@aarj.edu.eg, marah@aarj.edu.eg, u.murad@aarj.edu.eg.

Theoretical Studies of Thin-Film Solar Cells based on CdTe with different Window-Layers

H. A. Mohamed^{1,*}, Mahrous R. Ahmed¹, Sh. S. Ali¹ and W. S. Mohamed^{1,2}

¹ Physics department, Faculty of Science, Sohag University, 82524 Sohag, Egypt

² Physics Department, College of Science, Jouf University, Al-Jouf, Sakaka, P.O. Box 2014, Saudi Arabia

Received: 21 Feb. 2020, Revised: 22 Mar. 2020, Accepted: 24 Mar. 2020.

Published online: 1 Sep. 2020.

Abstract: The effect of using different types of window layer on the performance of thin-film solar cell based on CdTe was studied. Here, we investigated Cadmium Sulphide (CdS), Zinc Selenide (ZnSe) and Zinc Sulphide (ZnS) as window layer candidates. The calculations of short-circuit current density, internal quantum efficacy, external quantum efficient and the solar cell efficacy were achieved based on the optical and recombination losses. The calculation of the optical losses was performed considering the reflection process at the interfaces of the contacted layer and absorption process in the frontal charge-collecting and window layers. The recombination loss estimates on both front and back surfaces of the CdTe layer is based upon the physical parameters of the window/absorber junction and absorber layer. It was found that the highest short-circuit current density of 26 mA/cm², the lowest optical and recombination losses of 16% and consequently the highest cell efficiency of about 21.3% were achieved for ZnS window layer. For CdS window layer, the values of short-circuits current density, optical and recombination losses and cell efficiency were 23.38 mA/cm², 25% and 19%, respectively. The corresponding values of ZnSe layer were between those of ZnS and CdS. These results show that ZnS is considered a good alternative material for the traditional CdS window layer or at least it makes a promising alloy with CdS.

Keywords: CdTe thin-film solar cell; Window layers; Optical losses; Recombination losses.

1 Introduction

CdTe based thin-film photovoltaic is one of the most attractive and promising substrate thin-film solar cells. CdTe is an ideal absorber material for its 1.45 eV energy gap, which is ideal for solar energy conversion [1]. Moreover, CdTe has a high absorption coefficient so a few microns are sufficient to absorb more than 98 % of the light [2]. CdS and CdTe make an ideal junction for solar cell application because of the CdS-CdTe lattice similarities, which improve junction and device performance [3].

CdS material has unique physical and chemical properties such as superior transparency, direct band gap transition, minimal exciton Bohr radius of 2.5 nm, high electron affinity, n-type conductivity and thermal stability [4-6]. However, the 2.42 eV energy gap of CdS is comparatively low thus the photons with energy from 2.42 eV to end of visible region range are prevented to pass to absorber layer [7] and so causing little contribution to the photocurrent. Improvement the performance of CdTe solar cell can be introduced by replacing the traditional CdS

with wide band gap materials such as ZnS [8] and ZnSe [9] where they allow more light to pass without being absorbed.

ZnS is considered the better choice as a window layer because it has a wide direct energy gap (3.68 eV), environmentally safe, earth-abundance and cheapness. More transparency in wavelength range 350–550 nm could be achieved for ZnS material comparing with CdS [8]. ZnSe is an excellent substitute for CdS in photovoltaic solar cells because of its 2.7 eV wide band gap [9]. There are a lot of previous studies that are focusing on using different materials rather than CdS as a buffer layer for thin-film solar cells. It is reported that, using ZnS as a window layer lead to further improvement in the short current-density (J_{sc}) of CIGS thin-film solar cell [10, 11]. Hong et al [12] succeeded in using chemical bath deposition technique to fabricate ZnS/CIGS solar cell with reasonable efficiency and high open circuit voltage. Besides, ZnSe thin film was applied as a window layer successfully in thin-film solar cells based on CdTe [13] and CIGS [14]. Using the chemical bath deposition ZnSe buffer, a CIGS cell efficiency of 15.7% was achieved by Hariskos et al [15]. On the other hand, Mahajan et al [16]

*Corresponding author E-mail: hussein_abdelhafez2000@yahoo.com

reported on the different buffer layers fabrication of CZTS heterojunction solar cells. They tested different materials as buffer layers such as Cadmium Sulphide (CdS), Zinc Sulphide (ZnS) and Cadmium Zinc Sulphide ($\text{Cd}_{7.23}\text{Zn}_{2.77}\text{S}_{10}$). The lowest efficiency was achieved for CdS as a buffer layer and the highest one was observed for CdZS.

In this work, a model of studying the effect of using different window layers (CdS, ZnSe, ZnS) on the CdTe-based solar cells performance has been established. The inefficiencies in the reflection and absorption processes in window and charge-collecting layers have been estimated. Moreover, the losses due to recombination at front and back surface of CdTe layer have been investigated. The calculations of the optical losses are accomplished in the bases of the optical contents (n , k) of the used substances. While, the calculations of losses due to recombination are achieved based on the physical properties of the absorber layer and the junction.

2 Model

The typical structure of thin-film solar cell based on CdTe is glass/ITO/window layer /CdTe/Metal. In such a model, the absorber (CdTe) is a p-type, with an energy gap of 1.42 eV, the junction is established at the CdTe p-type and n-type (CdS, ZnSe, ZnS) interface and the charge-collecting layer is formed from ITO.

2.1. Optical Losses

The calculation of quantum efficacy of thin-film solar cells requires optical transmission $T(\lambda)$. $T(\lambda)$ is determined by reflections from the interface's air/ glass, glass/ITO, ITO/window layer, and window layer/CdTe as well as absorption in the ITO and window layers.

Reflection of incident light occurs between any two consecutive layers that have two different refractive indices (n_1 , n_2), and the coefficient of refractive (R) can be determined from the known formula [17]:

$$R_{12} = \left(\frac{n_1 - n_2}{n_1 + n_2} \right)^2 \quad (1)$$

For conductive materials, the refractive index takes the form:

$$n^* = n - ik \quad (2)$$

, where n is the refractive index and k is the extinction coefficient.

Therefore, Eq.1 can be written in the following form:

$$R_{12}(\lambda) = \frac{|n_1^* - n_2^*|^2}{|n_1^* + n_2^*|^2} = \frac{(n_1 - n_2)^2 + (k_1 - k_2)^2}{(n_1 + n_2)^2 + (k_1 + k_2)^2} \quad (3)$$

The values of optical constants of ITO, CdS, ZnSe, ZnS and CdTe were taken from the literature data [17, 18]. For substrate solar cells, the incoming light from air passes

through the substrate and then the other layers. In this case the reflectivity can occur at the air/glass interface. In our model, we assumed that the refractive index of glass varies with the wavelength according to the following equation [19]:

$$n^2 = 1 + \frac{a_1 \lambda^2}{\lambda^2 - \lambda_1^2} + \frac{a_2 \lambda^2}{\lambda^2 - \lambda_2^2} + \frac{a_3 \lambda^2}{\lambda^2 - \lambda_3^2} \quad (4)$$

Here, $a_1=0.6962$, $a_2=0.4079$, $a_3=0.8974$, $\lambda_1=68$ nm, $\lambda_2=116$ nm, and $\lambda_3=9896$ nm.

The transmission of light at normal incident and under the consideration of neglecting the apportion process is given by $T(\lambda)=1-R(\lambda)$. Therefore, $T(\lambda)$ of the system that consists of air/glass/ITO/window is given by:

$$T(\lambda) = (1 - R_{12})(1 - R_{23})(1 - R_{34})(1 - R_{45}) \quad (5)$$

where R_{12} is the reflection coefficient at air/glass interface, R_{23} is the reflection coefficient at glass/ITO interface, R_{34} is the reflection coefficient at ITO/window interface and R_{45} is the reflection coefficient at the window/CdTe interface.

When the absorption of the incident light is taking place in both ITO (with absorption coefficient α_1) and window layers (with absorption coefficient α_2), the transmission coefficient reads:

$$T(\lambda) = (1 - R_{12})(1 - R_{23})(1 - R_{34})(1 - R_{45})e^{-\alpha_1 d_1} e^{-\alpha_2 d_2} \quad (6)$$

where, d_1 and d_2 are the thickness of ITO and window layers, respectively.

The absorption coefficient $\alpha(\lambda)$ can be calculated using the formula:

$$\alpha = \frac{4\pi}{\lambda} k \quad (7)$$

where k is the wavelength-based extinction coefficient $k(\lambda)$.

The quantitative estimation of the optical losses (reflection) and its effect on the performance of solar cell can be done through the calculation of the short-circuit current density, J_{sc} , according to the following equation [20]:

$$J_{sc} = q \sum_i \frac{\Phi_i(\lambda_i)}{h\nu_i} T(\lambda_i) \Delta\lambda_i \quad (8)$$

where Φ_i is the spectral power density, $h\nu$ is the photon energy and $\Delta\lambda$ is the interval between neighbouring values of the wavelength.

We can determine the optical losses using Eq. (8) and the flowing expression

$$\text{Losses (\%)} = \left(1 - \frac{J_{sc}}{J_{sc(max)}} \right) \times 100 \quad (9)$$

where $J_{sc(max)}$ is the maximum short-circuit current density obtained at $T(\lambda) = 1$. The summation in Eq. (8) should be computed over the spectral range from $\lambda = 300$ nm to $\lambda = \lambda_g = hc/E_g$, where E_g is the optical band gap of CdTe. The interference effects in CdTe-based thin-film

solar cells is minimal, i.e. they hardly change the short circuit current [21]. Therefore, we neglected this effect in this study. Besides, it was found that [22] the multi reflections effect results in 1% transmission increase and J_{SC} increases by a very small value, indicating a weak effect of the multi reflection losses in enhancing the cell efficiency. Therefore, we neglected this effect in the current study.

2.2. Recombination Losses

Kosyachenko et al [23] simplified the expression of the quantum efficiency, which was given by Lavagna et al [24] to be in the following form.

$$\eta_{int} = \frac{1+(S_f/D_p)[\alpha+(2/W)(\phi_o-qV)/kT]^{-1} - \exp(-\alpha W)}{1+(S_f/D_p)[(2/W)(\phi_o-qV)/kT]^{-1} + \alpha L_n} \quad (10)$$

where S_f is the recombination velocity, D_p is hole diffusion coefficient, α is the absorption coefficient, W is the width of depletion region, and ϕ_o is the barrier height, $L_n (= \tau_n D_n)$ is diffusion length of minority carriers, τ_n is the lifetime of electron and D_n is the diffusion coefficient of the electrons. D_p and D_n are calculated by the Einstein relation $qD_r/kT = \mu_r$, where r is the carrier mobility.

The known Gartner formula can be obtained by the following expression by putting $S_f=0$ in Eq. (10) [25]:

$$\eta_{int} = 1 - \frac{\exp(-\alpha W)}{1 + \alpha L_n} \quad (11)$$

The quantum yield that takes place in the depletion region equals the absorptivity (i.e., $1 - \exp(-\alpha W)$). Thus, on subtracting the term $1 - \exp(-\alpha W)$ from the right side of Eq. (10), we obtain the diffusion component of the photoelectric quantum yield:

$$\eta_{diff} = \exp(-\alpha W) \frac{\alpha L_n}{1 + \alpha L_n} \quad (12)$$

This equation ignores the recombination at the back surface of the absorber layer. On subtracting the right side of Eq. (12) from the right side of Eq. (10) we obtain the drift component of the photoelectric quantum yield: $\eta_{drift} = \frac{1+(S_f/D_p)[\alpha+(2/W)(\phi_o-qV)/kT]^{-1}}{1+(S_f/D_p)[(2/W)(\phi_o-qV)/kT]^{-1} + \alpha L_n} - \exp(-\alpha W)$ (13)

The drift component of the photoelectric quantum yield takes into account surface recombination at the front interface, while the diffusion component of the internal quantum efficiency includes the recombination losses at back surface of the absorber, which takes the form [26]:

$$\eta_{dif} = \frac{\alpha L_n}{\alpha^2 L_n^2 - 1} \exp(-\alpha W) \times \left\{ \alpha L_n - \frac{\left(\frac{S_b L_n}{D_n}\right) [\cosh((d-W)/L_n) - \exp(-\alpha(d-W))] + \sinh((d-W)/L_n) + \alpha L_n \exp(-\alpha(d-W))}{\left(\frac{S_b L_n}{D_n}\right) \sinh((d-W)/L_n) + \cosh((d-W)/L_n)} \right\} \quad (14)$$

where S_b is the back-surface recombination speed and the absorber thickness is denoted by d . From Eq. (13) and Eq.

(14), the total internal quantum efficiency with recombination losses at front and back surface of the absorber layer is:

$$\eta_{int} = \eta_{drift} + \eta_{dif} \quad (15)$$

The quantitative effect of the recombination losses on the J_{SC} can be given using Eq.(8) but in the following form:

$$J_{SC} = q \sum_i \frac{\Phi_i(\lambda_i)}{h\nu_i} \eta_{int}(\lambda_i) \Delta\lambda_i \quad (16)$$

In this case, Eq. (9) is used to calculate the recombination losses, where $J_{SC(max)}$ is obtained at $S_f=0$ and $S_b=0$.

According to Eqs. (13)-(16), $J_{SC(max)}$ depends mainly only on d and W . The other data that are represented in Eqs. (14) and (15) are used in this model are reported in Table 1.

The external quantum efficiency η_{ext} can be calculated utilizing internal quantum efficiency as:

$$\eta_{ext} = T(\lambda) \eta_{int} \quad (17)$$

where $T(\lambda)$ is given by Eq. (6), which takes into account the optical losses.

2.3. Solar Cell Parameters

The current density $J(V)$ of a solar cell with single junction under illumination, may be formulated as a function of the dark and photo currents as:

$$J = J_0 \left[\exp\left(\frac{qv}{AkT}\right) - 1 \right] - J_L \quad (18)$$

where J_L is the photogenerated current, J_0 is the reverse saturation current, q is the elementary charge, k the Boltzmann constant, T the absolute temperature and A the ideality factor. The value of J_0 is taken from [27].

The efficiency of solar cell efficiency is given by:

$$\eta = \frac{FF \times J_{SC} \times V_0}{P_{in}} \quad (19)$$

where FF is the fill factor, V_0 is the open circuit voltage, P_{in} (100 mW/cm²) is the power density of the total AM 1.5 solar radiation.

The fill factor can be written as:

$$FF = \frac{J_m \times V_m}{J_{SC} \times V_0} \quad (20)$$

where J_m and V_m are the maximum current density and voltage, respectively. In this model, we assume that $J_L = J_{SC}$.

J_{SC} in the case of both optical and recombination losses are given from:

$$J_{SC} = q \sum_i \frac{\Phi_i(\lambda_i)}{h\nu_i} T(\lambda) \eta_{int}(\lambda_i) \Delta\lambda_i \quad (21)$$

Using this expression with Eq. (9), the optical and recombination losses can be computed.

3 Results and Discussion

Figure 1 indicates the effect of window layer (CdS, ZnSe, ZnS) on the reflection coefficient $R(\lambda)$. It can be seen that the values of $R(\lambda)$ are in the range from 0.01 to 0.04 for the

Table 1. The used parameters in this model.

Parameter	d_{ITO}	$\phi_0 - qV$	S_n	S_p	μ_n	μ_p	τ_n	T
Value	100 (nm)	1 (eV)	10^7 (cm/s)	10^7 (cm/s)	10^3 cm ² /(Vs)	10^2 cm ² /(Vs)	10 (ns)	300(K)
Ref.	[21, 26]	[17]	[17]	[17,21, 26]	[17,21, 26]	[17,21, 26]	This work	This work

interface between ITO and the window layer (i.e. ITO/CdS, ITO/ZnSe, ITO/ZnS) as shown in Fig.1-a. For the interface between window layer and the absorber layer (i.e. CdS/CdTe, ZnSe/CdTe, ZnS/CdTe), the values of $R(\lambda)$ are also small and are in the range from 0.05 to 0.065 as shown in Fig.1-b. The behaviour of these curves depends mainly on the variation of optical constants (n , k) of the used materials with wavelength. These low values of reflection coefficient are due to a relatively small difference between the optical constants (n , k) of contacting materials [17].

Figure 2 illustrates the dependence of transmission coefficient $T(\lambda)$ on the thickness of each window layer (CdS, ZnSe, ZnS). The results are carried out using Eq. (6), which takes into consideration the reflection at various interfaces and the absorption in ITO and window layer. While the thickness of ITO layer is 100 nm, the thicknesses of window layers are varied from 50 nm to 150 nm. It can be seen that a small decrease in $T(\lambda)$ is observed at λ greater than 550 nm. And a great decrease in $T(\lambda)$ can be observed at $\lambda < 500$ nm caused by absorption in both ITO and window layer. Moreover, with increasing the thickness of window layer, more decrease in $T(\lambda)$ can be observed.

The dependence of $T(\lambda)$ on the thickness of window layer is clear in the case of CdS (Fig.2-a) and this dependence becomes unclear for ZnSe (Fig.2-b) and ZnS (Fig.2-c) particularly at long wavelength, indicating a weak effect of the thickness of ZnSe and ZnS on the spectral transmission. The replacement of the window material (CdS) with wide band gap materials (ZnSe, ZnS) resulted in enhancing the transmission properties of the multilayer system. For 50 nm thickness of CdS, ZnSe, and ZnS the average of $T(\lambda)$ is 0.58, 0.63, 0.76, respectively. Besides, it is difficult to decrease the window layer thickness to less than 50 nm to avoid the pin-hole effect that takes place in thin thickness [27].

Equations (8) and (9) are employed to calculate the short-circuit current density and the corresponding optical losses and the results are plotted in Fig.3-a. As seen from this figure, J_{SC} decreases with increasing the thickness of the window layer. As understand

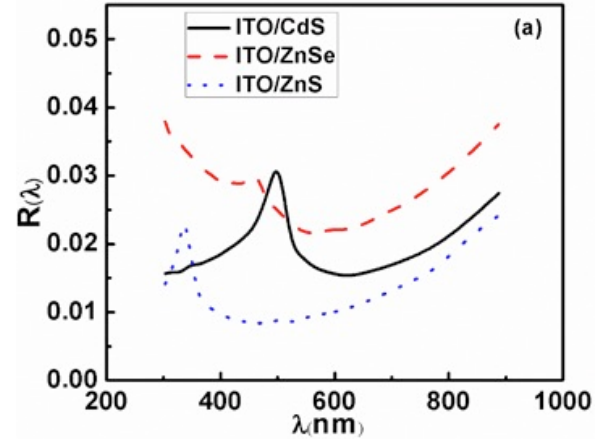
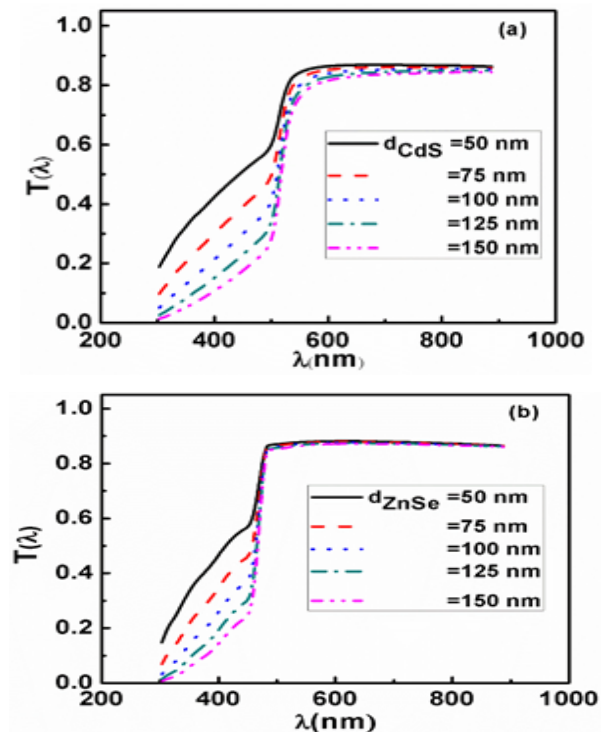


Fig.1: Spectral reflection coefficient (R) at the interfaces ITO/window layer (CdS, ZnSe, ZnS) (a) and at interfaces window layer (CdS, ZnSe, ZnS)/CdTe (b).



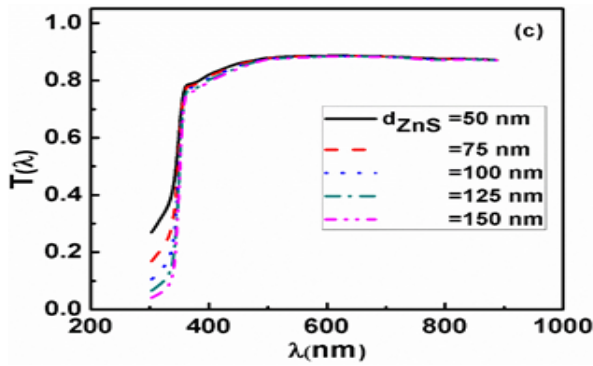


Fig.2: Spectral transmission coefficient (T) as a function of the thickness of window layer CdS(a), ZnSe (b) and ZnS (c).

from Eq. (8), the transmission is the only effect on J_{SC} values. The maximum J_{SC} value of more than 27 mA/cm² is obtained for ZnS window layer at thickness of 50 nm and the minimum value of about 25 mA/cm² is obtained for CdS window layer at the same thickness. These due to the decreasing of energy gape from ZnS to CdS materials. Besides, the increase of the thickness of the window layer leads to decrease in J_{SC} values due to the absorption process that takes place in this layer. The optical losses as shown in Fig. 3-b represent a reverse behaviour of that obtained in Fig.3-a. For ZnS, the optical losses are around 12.8 % and these losses increase with decreasing the energy gap and the thickness of the window layer. The maximum optical losses record is 32% for CdS at thickness of 150 nm, indicating that a significant amount of light will not reach the absorber layer.

The above values of J_{SC} can be used in Eq. (18) to study the I - V curve of solar cell for different window layers with different thickness as shown in Fig.4. As seen from this figure, with increasing the thickness of the window layer the curves shift upward due to the decreasing in J_{sc} and this behaviour is more obviously for CdS window layer which is matching with the results obtained in Figs. 2 and 3. It can be seen that, the values of V_{OC} for each window layer is approximately constant because we used the same value of the reverse saturation current J_0 and idialty factor A as mentioned in Ref. [27].

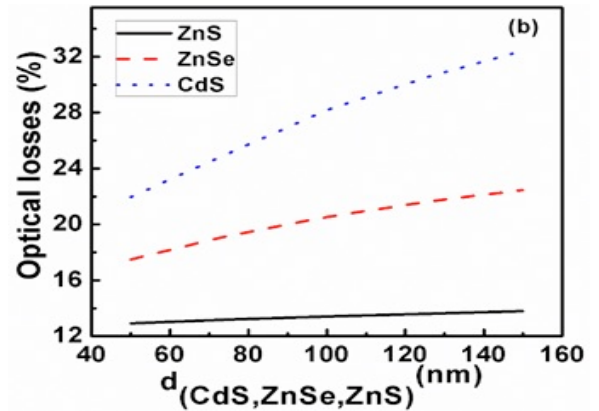
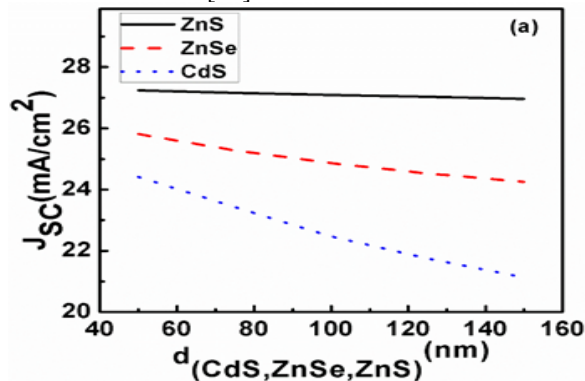


Fig.3: Calculated short-circuit current density (J_{sc}) as function of the thickness of window layer (CdS, ZnSe, ZnS) (a) and the corresponding optical losses (b).

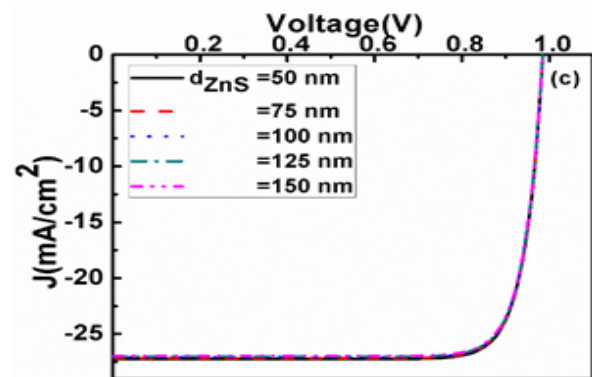
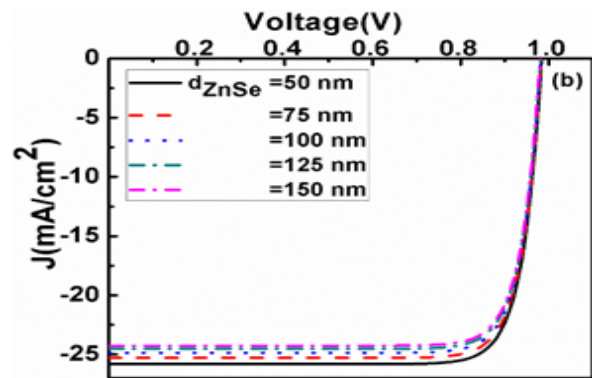
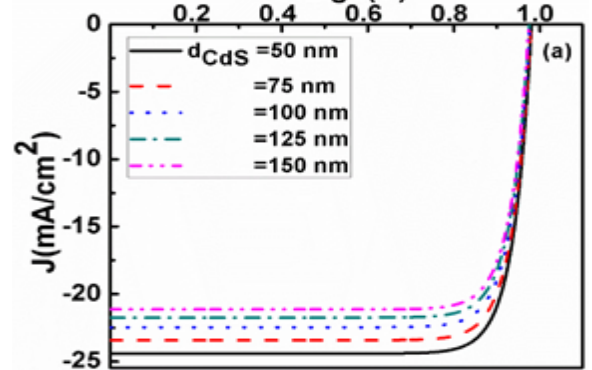


Fig.4: J - V characteristic curve at various values of the thickness of window layer CdS (a), ZnSe (b) and ZnS (c).

Figure 5 represents the solar cell efficiency of each window layer as a function of the layer thickness. Similar behaviour of current density is witnessed for efficiency where the gradient for the CdS layer is steeper than ZnSe and ZnS. As expected, ZnS shows the highest efficiency more than 22 % and this efficiency is approximately independent on the thickness of ZnS. For ZnSe the efficiency is smaller than that of ZnS and the influence of thickness is clear where the minimum efficiency of 20 % is achieved at 150 nm thickness. Finally, CdS shows the smallest efficiency comparing with ZnS and ZnSe and this efficiency can reach 17% at 150 nm thickness. The analysis of the results presented in Fig.5 in terms of optical losses indicates that the most appealing structure at the investigated thicknesses is ZnS/CdTe. On the other hand, the worst structure in the auxiliary layers is the traditional CdS/CdTe. While, the containing ZnSe window layer exhibited the intermediate behaviour between these structures. The similar results were achieved for the absorber layer $\text{Cu}_2\text{ZnSn}(\text{S,Se})_4$ [18].

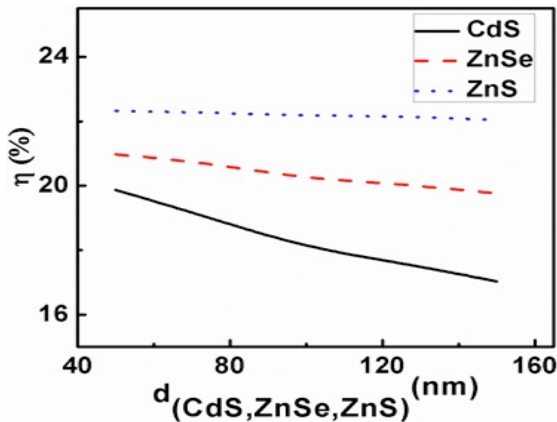


Fig.5: Efficiency of CdTe thin-film solar cell at different thicknesses of window layer (CdS, ZnSe, ZnS) under the influence of optical losses.

The analysis of internal quantum efficiency, η_{int} , given by Eqs. (13)-(15) shows that the important parameters are the width of space charge region (W) and the thickness of the absorber layer (d). Accordingly, Fig.6 shows the dependence of spectral internal quantum efficiency, η_{int} , on the width of space-charge region (Fig.6-a) at fixed thickness of CdTe ($5\mu\text{m}$) and the dependence of η_{int} on the thickness of CdTe at fixed $W=0.7\mu\text{m}$ (Fig.6-b). As seen from Fig.6-a, η_{int} increases with increasing W and maintains a constant behaviour at higher values of W , due to the fact that at higher values of W more photons are absorbed in the space-charge region. At wide W , the formed electric field in space-charge region becomes weaker and no more increase in η_{int} can be observed. It is observed that the internal quantum efficiency reaches its maximum value when W reaches $0.7\mu\text{m}$. In this case the recombination losses record the value of 2 %. In addition, η_{int} increases with increase the

thickness of CdTe particularly at long wavelength and no more significant effect can be observed at higher thickness. It can be seen that the thickness of CdTe in the range $6\text{-}8\mu\text{m}$ is sufficient to absorb most the incident light and the recombination losses in this case are 1%. Comparing Fig. 6-a with Fig.6-b, we can conclude that the width of the space-charge region is more effective than the thickness of the absorber layer.

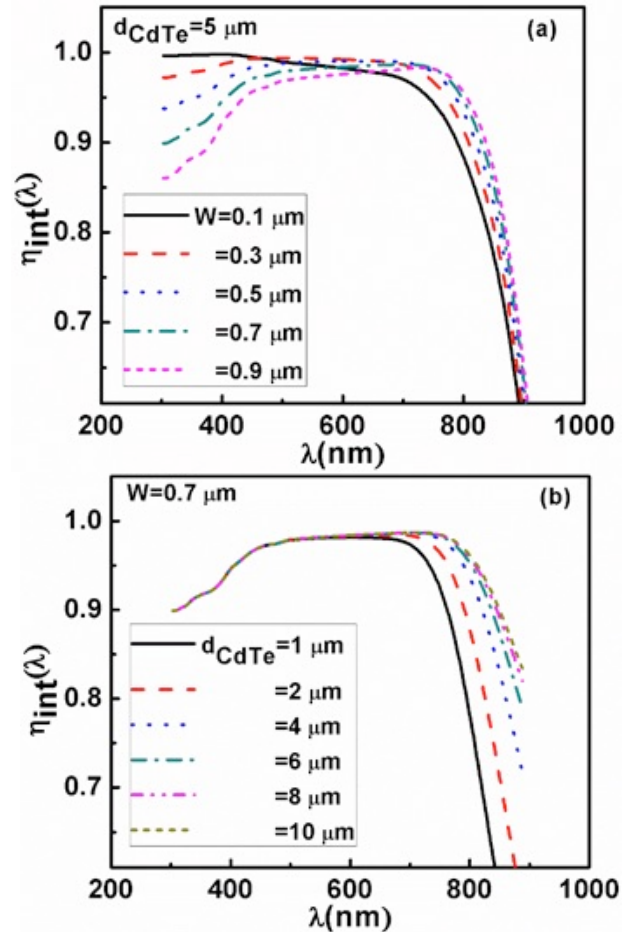


Fig.6: Spectral internal quantum efficiency (η_{int}) at different values of the width of space charge region (W) (a) and at different thicknesses of CdTe (d_{CdTe}) (b).

The values of internal quantum efficiency as a function of the width of space-charge region and of the thickness of the absorber are employed in Eq. (16) to evaluate the short-circuit current density and consequently estimate the value of cell efficiency as shown in Fig.7. It is clear that J_{sc} increases with increasing d_{CdTe} until $7\mu\text{m}$ thickness. With further increase in thickness, J_{sc} does not appear a significant dependence on the absorber thickness. Besides, J_{sc} increases also with increasing the width of space-charge region and no further increase can be achieved at $W > 0.5\mu\text{m}$. As shown in Fig.7-b, the maximum cell efficiency can exceed 24.7% under the influence of the recombination losses at front and back surface of CdTe.

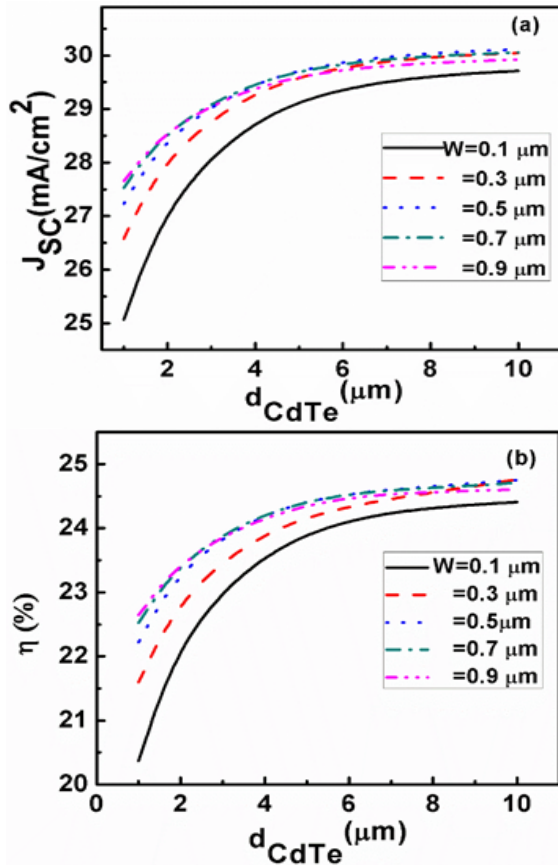


Fig.7: Calculated short-circuit current density (J_{sc}) as function of the thickness of CdTe (d_{CdTe}) at different values of the width of space-charge region (W) (a) and the corresponding cell efficiency (η) (b).

Fig. 8 shows the spectral external quantum efficiency given by Eq. (17) and that takes into consideration the optical losses. The value and behaviour of η_{ext} differs from those obtained for η_{int} due to the reflection at interfaces as well as the absorption in window layer. The results of this figure are carried out as a function of the thickness of absorber at $W=0.7 \mu\text{m}$ and thickness of 75 nm of the window layer. This figure seems to be a combine with Fig. 2 and Fig. 6-b. It can be observed that, η_{ext} increases with increase d_{CdTe} particularly at long wavelength and no further increase can be achieved at higher thicknesses.

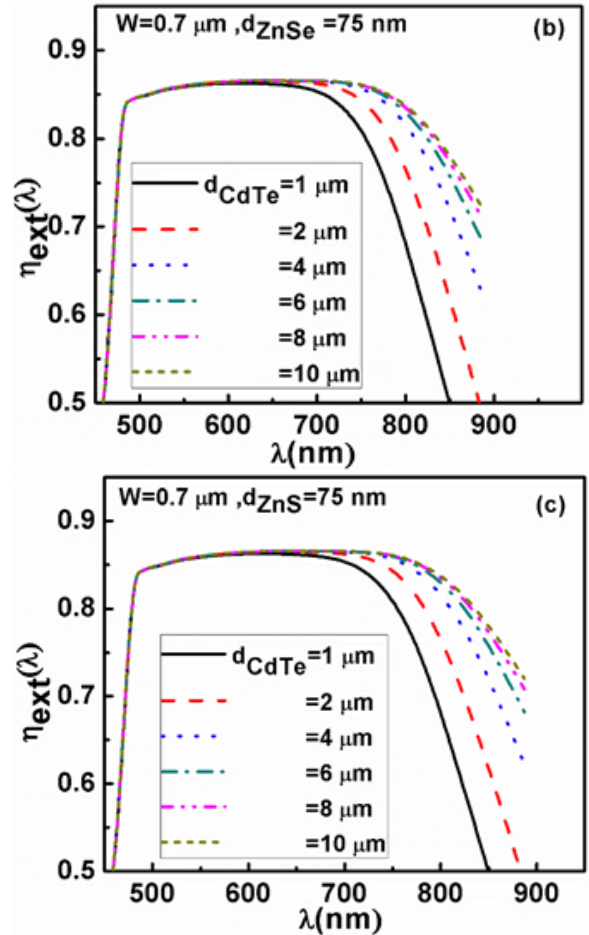
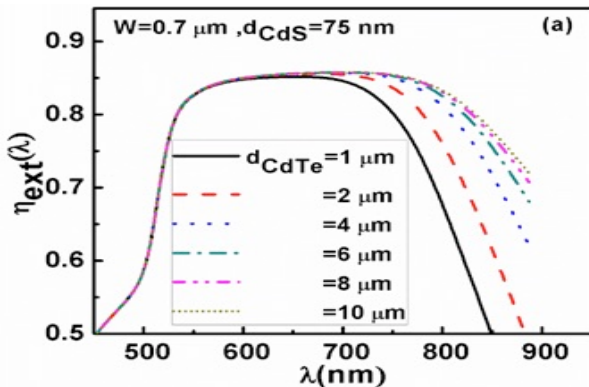


Fig.8: Spectral external quantum efficiency (η_{ext}) at different thicknesses of CdTe (d_{CdTe}) for CdS(a) ZnSe (b) and ZnS (c).

In order to achieve realistic parameters of CdTe solar cell, both the optical and recombination losses should be taken in calculations. Accordingly, Eq. (21) is used to calculate J_{SC} and the results are plotted in Fig.9-a. The results of this figure are carried out at $W=0.7 \mu\text{m}$ and $d_{CdTe}=5 \mu\text{m}$. As expected, J_{SC} decreases with increasing the thickness of window layer where more photon can be absorbed. At thickness of 60 nm, J_{SC} records the values 26 mA/cm², 24.3 mA/cm² and 22.8 mA/cm² for ZnS, ZnSe and CdS respectively. At these values, the corresponding optical and recombination losses are 16%, 20.5% and 24.7 %, respectively as shown in Fig.9-b. Besides, we can observe that these losses become more effective at higher thicknesses of the window layer and can be increased by about 41.5% for increasing d_{CdS} from 50 nm to 150 nm. In the case of ZnS, these losses increased only by about 5.3% which represents the importance of using material as an alternative window layer of CdS.

Finally, the efficiency of thin-film solar cells based on CdTe at various window layers is calculated and plotted in Fig. 10 under the influence of optical and recombination losses. As seen from this figure at small thickness of the

window layer, ZnS shows a highest efficiency comparing with the other layers which is more than 21% and CdS shows the lowest efficiency of about 19%. Besides, ZnSe represents a 20 % efficiency which is intermediate between ZnS and CdS.

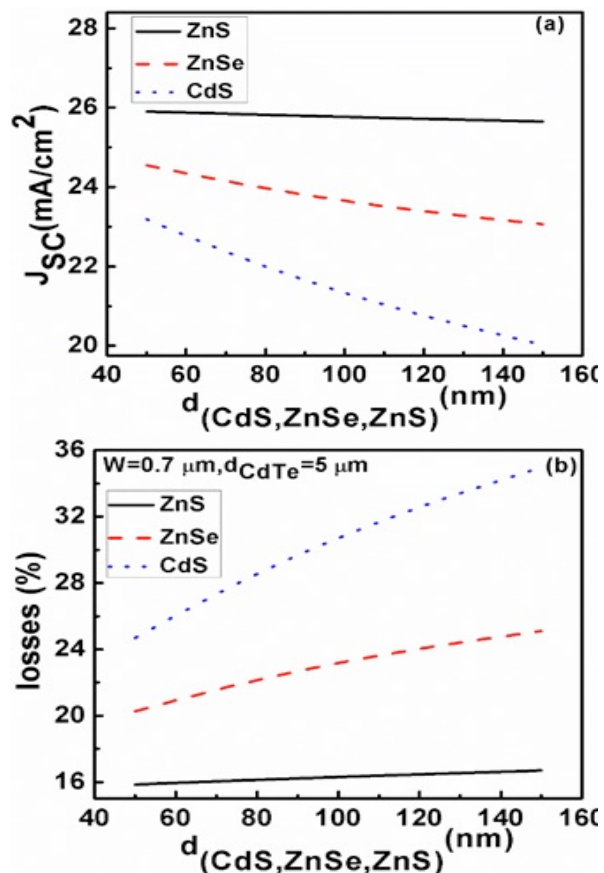


Fig.9: Calculated short-circuit current density (J_{sc}) as function of the thickness of window layer (CdS, ZnSe and ZnS) (a) and the corresponding optical and recombination losses (b).

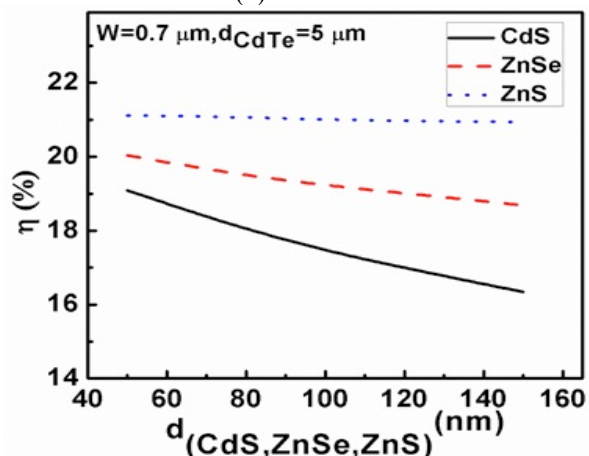


Fig.10: Efficiency of CdTe thin-film solar cell at different thicknesses of window layer (CdS, ZnSe, ZnS) under the influence of optical and recombination losses.

4 Conclusions

We investigated the effect of using different materials of CdS, ZnSe and ZnS as window layer for CdTe based thin-film solar cells. In this work, the influence of optical and recombination losses on the performance of CdTe solar cells was studied. The calculations of optical losses were achieved based on the reflection at various interfaces and absorption in both frontal charge-collecting layer (ITO) and window layer. The calculations of the recombination losses were based on the recombination at front and back surfaces of CdTe. The values of short-circuit current density and quantum efficiency when using ZnS as a window layer were higher than those of ZnSe and CdS. The lowest losses of 16 % were obtained for ZnS material and these losses increased up to 24 % in the case of CdS. ZnS showed a highest efficiency which is more than 21%, CdS showed the lowest efficiency of about 19%, while ZnSe represented a 20 % efficiency which is intermediate between ZnS and CdS.

Conflicts of Interest: The authors declare that they have no conflict of interest.

Data availability statement: The data that support the findings of this study are available from the corresponding author upon reasonable request.

References

- [1] Sharma, R.K., Jain, K. and Rastogi, A.C. (2003) Growth of CdS and CdTe Thin Films for The Fabrication of n-CdS/p-CdTe Solar Cell. *Current Applied Physics.*, **3**, 199-204(2003).
- [2] L. A. Kosyachenko, X. Mathew, V. Ya.Roshko, E. V. Grushko, *Solar Energy Materials & Solar Cells.*, **114**, 179–185(2013).
- [3] Songwei Liu, Weigeng Liu, JingxuanHeng, Wenfeng Zhou, Yanru Chen, Shiya Wen, Donghuan Qin, LintaoHou, Dan Wang and Hui Xu, *Coatings.*, **8**, 1(2018).
- [4] G. Perna, V. Capozzi, M. Ambrico, V. Augelli, T. Ligonzo, A. Minafra, L. Schiavulli, M. Pallara, Structural and optical characterization of undoped and indium-doped CdS films grown by pulsed laser deposition, *Thin Solid Films.*, **453e454**, 187-194(2004).
- [5] A.S. Opanasyuk, D.I. Kurbatov, M.M. Ivashchenko, I.Y. Protsenko, Properties of the window layers for the CZTSe and CZTS based solar cells, *J. NanoElectron. Phys.*, **4(1)** (2012) 01024, 3pp.
- [6] Ligang Ma, Xiaoqian Ai, Xiaoshan Wu, *Journal of Alloys and Compounds .*, **691**, 399-406(2017).
- [7] J. Han, C. Liao, T. Jiang, C. Spanheimer, G. Haindl, G. Fu, V. Krishnakumar, K. Zhao, A. Klein, W. Jaegermann, An optimized multilayer structure of CdS layer for CdTe solar cells application, *J. Alloys Compd.*, **509**, 5285-5289(2011).
- [8] Z. Y. Zhong, E. S. Cho, S. J. Kwon, et al., *Mater. Chem. Phys.*, **135**, 287–292(2012).

- [9] M. Moradi, R. Teimouri, M. Saadat, M. Zahedifar, *Optik.*, **136**, 222–227(2017).
- [10] T. Nakada, M. Mizutani, *Jpn. J. Appl. Phys.*, **41**, L165(2002).
- [11] T. Kobayahi, H. Yamaguchi, T. Nakada, *Prog. Photovoltaics: Res. App.*, **22**, 115(2014).
- [12] J. Hong, D. Lim, Y. J. Eo, Changhwan Choi, *Applied Surface Science.*, **432**, 250(2017).
- [13] Acharya, S.; Bangera, K.V.; Shivakumar, G.K. Electrical characterization of vacuum-deposited p-CdTe/n-ZnSe heterojunctions. *ApplNanosci.*, **5**, 1003–1007(2015).
- [14] A. Shimizu, S. Chaisitsak, T. Sugiyama, A. Yamada, and M. Kongai, *Thin Solid Films*, 361-362: 193-197 (2002).
- [15] D. Hariskos, S. Spiering, and M. Powalla, *Thin Solid Films.*, **99**, 480-481(2005).
- [16] S. Mahajan, D. Sygkridou, E. Stathatos, N. Huse, A. Kalarakis, R. Sharm, *Superlattices and Microstructures.*, **109**, 240-248(2017).
- [17] H. A. Mohamed, *J. Appl. Phys.*, 113, 093105(2013)
- [18] O. A. Dobrozhan, P. S. Danylchenko, A. I. Novgorodtsev, and A. S. Opanasyuk, *Journal of Nanoelectronics and Optoelectronics.*, **12**, 1–13(2017).
- [19] S. O. Kasap, *Optoelectronics and Photonics: Principles and Practice* (Prentice-Hall, New Jersey., 45(2000).
- [20] H. A. Mohamed, A. S. Mohamed and H. M. Ali, *Mater. Res. Express.*, **5**, 056411(2018)
- [21] L.A. Kosyachenko, E.V.Grushko, X. Mathew, *Solar Energy Materials & Solar Cells* ., **96**, 231–237(2012).
- [22] H. A. Mohamed and N.M.A. Hadia, *Optik.*, **126**, 1976–1980(2015)
- [23] Kosyachenko, L.A., Sklyarchuk, V.M., Sklyarchuk, Ye.F. &Ulyanitsky, K.S. (1999). Surfacebarrier p-CdTe-based photodiodes, *Semicond. Sci. Technol.*, **14**, 373-377(1999).
- [24] Lavagna, M., Pique, J.P. &Marfaing, Y. (1977). Theoretical analysis of the quantum photoelectric yield in Schottky diodes, *Solid State Electronics.*, **20**, 235-240(1977)
- [25] Gartner W.W., (1959). Depletion-layer photoeffects in semiconductors, *Phys. Rev.*, **116**, 84-87(1959).
- [26] L. A. Kosyachenko, X. Mathew, P. D. Paulson, V. Ya. Lytvynenko, O. L. Maslyanchuk, *Solar Energy Materials & Solar Cells.*, **130**, 291–302(2014).
- [27] J. H. Yun, E. S. Cha, B. T. Ahn, H. Kwon, E. A. Al-Ammar, *Current Applied Physics.*, **14**, 630e635(2014).